AGU PUBLICATIONS

Geophysical Research Letters

RESEARCH LETTER
10.1002/2013GL058942

Special Section:
Early Results From the Van Allen Probes

Key Points:
- Clear observations to higher energy than ever before
- Precise detection of where and how acceleration takes place
- Provides "new eyes" on megaelectron Volt

Correspondence to:
D. N. Baker,
Daniel.Baker@LASP.colorado.edu

Citation:
Baker, D. N., et al. (2014), Gradual diffusion and punctuated phase space density enhancements of highly relativistic electrons: Van Allen Probes observations, *Geophys. Res. Lett.*, *41*, 1351–1358, doi:10.1002/2013GL058942.

Received 22 DEC 2013
Accepted 13 JAN 2014
Accepted article online 15 JAN 2014
Published online 4 MAR 2014

Gradual diffusion and punctuated phase space density enhancements of highly relativistic electrons: Van Allen Probes observations

D. N. Baker[1], A. N. Jaynes[1], X. Li[1], M. G. Henderson[2], S. G. Kanekal[3], G. D. Reeves[2], H. E. Spence[4], S. G. Claudepierre[5], J. F. Fennell[5], M. K. Hudson[6], R. M. Thorne[7], J. C. Foster[8], P. J. Erickson[8], D. M. Malaspina[1], J. R. Wygant[9], A. Boyd[4], C. A. Kletzing[10], A. Drozdov[11], and Y. Y. Shprits[11,12,13]

[1]Laboratory for Atmospheric and Space Physics, University of Colorado Boulder, Boulder, Colorado, USA, [2]Los Alamos National Laboratory, Los Alamos, New Mexico, USA, [3]NASA/Goddard Space Flight Center, Greenbelt, Maryland, USA, [4]Institute for the Study of Earth, Oceans, and Space, University of New Hampshire, Durham, New Hampshire, USA, [5]Space Sciences Department, Aerospace Corporation, El Segundo, California, USA, [6]Department of Physics and Astronomy, Dartmouth College, Hanover, New Hampshire, USA, [7]Department of Atmospheric and Oceanic Sciences, University of California, Los Angeles, California, USA, [8]Haystack Observatory, Massachusetts Institute of Technology, Westford, Massachusetts, USA, [9]Department of Physics and Astronomy, University of Minnesota, Minneapolis, Minnesota, USA, [10]Department of Physics and Astronomy, University of Iowa, Iowa City, Iowa, USA, [11]Department of Earth Space Sciences, University of California, Los Angeles, California, USA, [12]Department of Earth Atmospheric and Planetary Sciences, Massachusetts Institute of Technology, Cambridge, Massachusetts, USA, [13]Skolkovo Institute of Science and Technology, Skolkovo, Russia

Abstract The dual-spacecraft Van Allen Probes mission has provided a new window into mega electron volt (MeV) particle dynamics in the Earth's radiation belts. Observations (up to E ~10 MeV) show clearly the behavior of the outer electron radiation belt at different timescales: months-long periods of gradual inward radial diffusive transport and weak loss being punctuated by dramatic flux changes driven by strong solar wind transient events. We present analysis of multi-MeV electron flux and phase space density (PSD) changes during March 2013 in the context of the first year of Van Allen Probes operation. This March period demonstrates the classic signatures both of inward radial diffusive energization and abrupt localized acceleration deep within the outer Van Allen zone (L ~4.0 ± 0.5). This reveals graphically that both "competing" mechanisms of multi-MeV electron energization are at play in the radiation belts, often acting almost concurrently or at least in rapid succession.

1. Introduction

From the earliest spacecraft observations [e.g., *Van Allen et al.*, 1958], it has been evident that the magnetic field region surrounding the Earth is capable of entraining intense populations of high-energy electrons and ions. These particle populations wax and wane in absolute flux on a wide range of timescales having both to do with internal magnetospheric physical processes and with external driving effects imposed by the solar wind [e.g., *Baker and Blake*, 2012].

The Radiation Belt Storm Probes (RBSP) mission was launched by NASA on 30 August 2012 in order to better understand radiation belt acceleration, transport, and loss processes [*Mauk et al.*, 2012]. Within days after their successful orbital insertion, the dual RBSP spacecraft (later renamed the Van Allen Probes) began to reveal new and unexpected things about the structure and dynamics of the Earth's radiation belts, including the existence of a third Van Allen belt dubbed the relativistic electron "storage ring" [*Baker et al.*, 2013; *Thorne et al.*, 2013a; *Shprits et al.*, 2013].

In this paper we present an inclusive overview of the first year of relativistic electron data acquired by Van Allen Probes instruments. We show the clear tendency for long periods of gradual radial transport and related electron loss during times when solar wind drivers were relatively quiescent. We also show numerous examples of abrupt losses of relativistic electrons, often followed by almost as abrupt resurgences of particle populations. We focus particular attention on a month-long interval in March 2013 when the magnetosphere showed a rich variety of phenomena. In the space of a few weeks during this time, there was a clear and

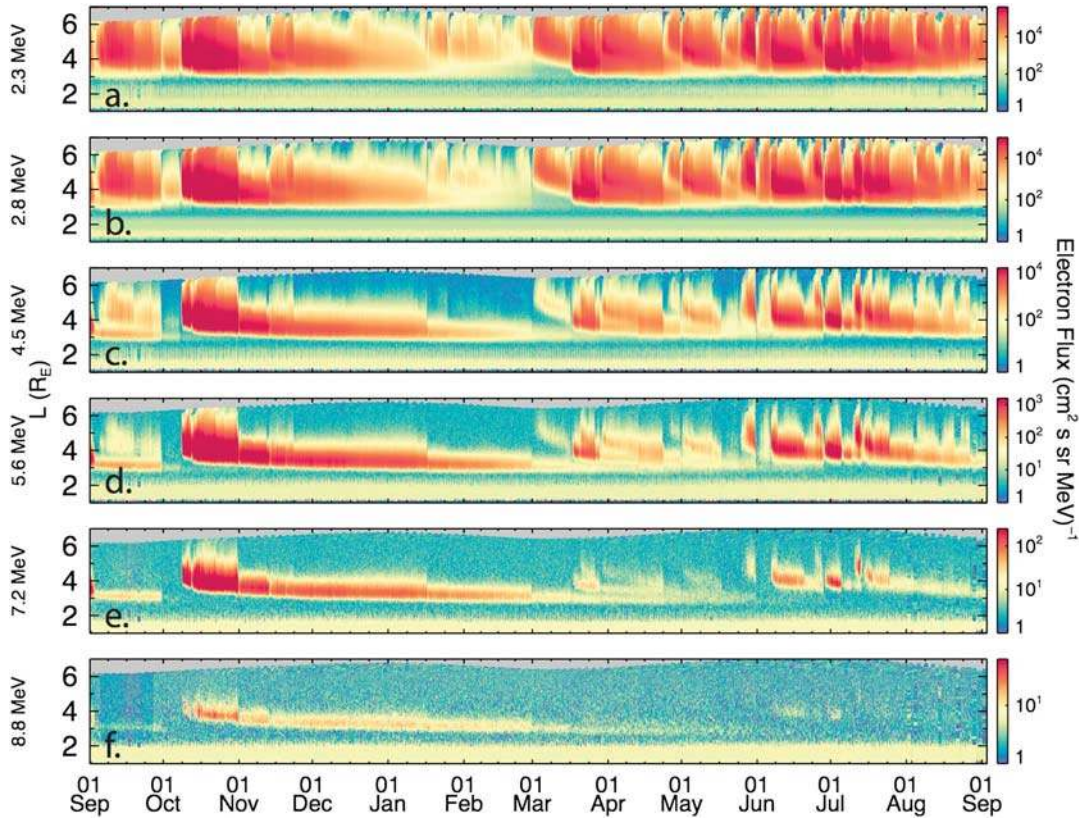

Figure 1. Color-coded fluxes of relativistic electron in an *L* versus time format in selected energy channels for the first year of Van Allen Probes operation (September 2012 to September 2013).

pronounced rapid inward radial transport of multi-MeV electrons from beyond 6 Earth radii (R_E) to 3 R_E geocentric distance or less. After the almost "surgical" removal of this high-energy particle population from the outer belt on 17 March, the magnetosphere revealed its ability to rapidly regenerate electrons up to E ~8 MeV on timescales of at most a few hours. In this way, we see that there clearly is a cosmic particle accelerator operating in Earth's immediate vicinity that is capable of remarkable efficiency and effectiveness. This paper explores the duality of gradualism and punctuated transitions using the new "eyes" that the Van Allen Probes provide.

2. Overview of the Radiation Belts: The First Year of Van Allen Data

The Van Allen Probes spacecraft each have a comprehensive particles and fields instrument payload on board [e.g., *Mauk et al.*, 2012]. In the present paper, we focus on medium to very high-energy electrons measured by the Relativistic Electron-Proton Telescope (REPT) investigation [*Baker et al.*, 2012]. The identical REPT instruments on board the RBSP-A and RBSP-B spacecraft measure electrons from E ~1.5 MeV to E ~20.0 MeV. The REPT large geometric factor (0.2 cm^2 sr), good background rejection, and outstanding intercalibration assure that radiation belt properties can be accurately assessed across the "slot" region and throughout the outer Van Allen zone with excellent temporal, spatial, and energy resolution [*Baker et al.*, 2012].

Figure 1 shows a year-long survey of data from the combined REPT-A and REPT-B investigations from initial instrument turn-on: 1 September 2012 to 1 September 2013. Each panel is plotted as color-coded electron flux values. The data are shown as a function of *L* on the vertical axis and time along the horizontal axis. (Here *L* is the distance in Earth radii at which a magnetic flux tube crosses the magnetic equatorial plane in a dipole magnetic field model). Each panel has its own logarithmic flux color bar, with (obviously) much higher electron intensities typically being measured in the lower energy range ($2.0 \le E \le 2.5$ MeV, Figure 1a), for example, than in the higher energy range ($7.7 \le E \le 9.6$ MeV, Figure 1f). Each panel shows electron measurements from L ~1.0 to L ~6.5 as

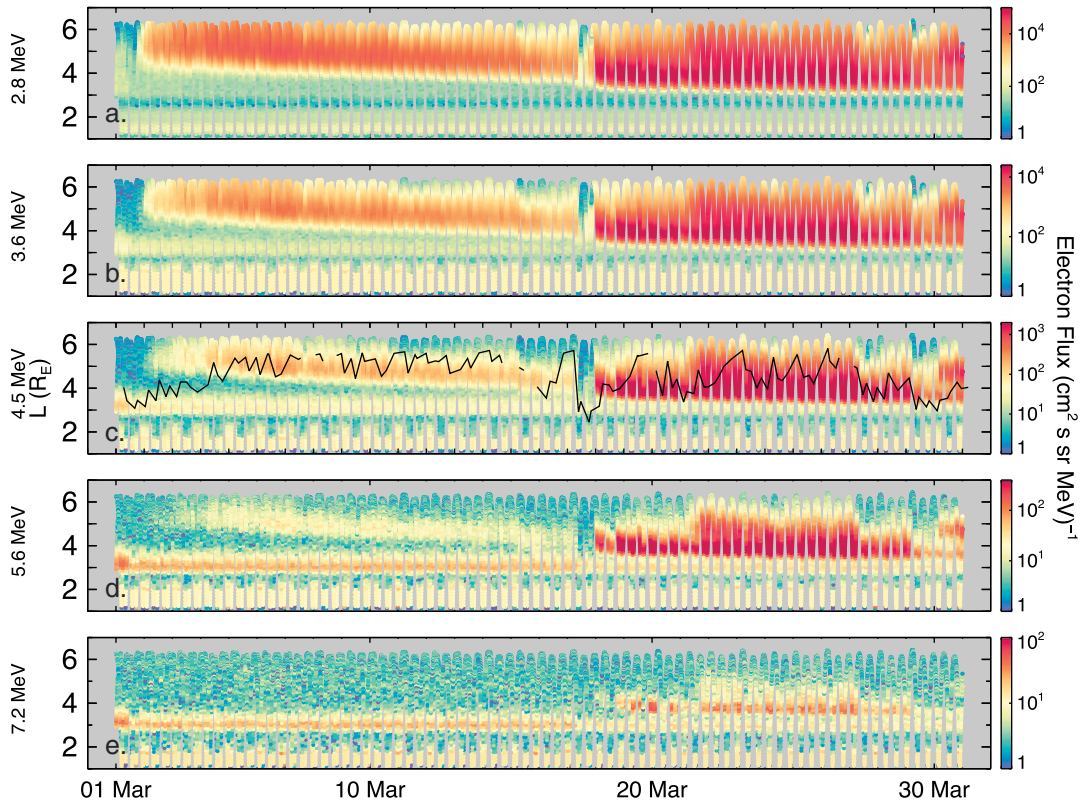

Figure 2. Details of multi-MeV electron flux variations (see Figure 1) for the month of March 2013. The black trace on Figure 2c represents the plasmapause location derived from EFW spacecraft density measurements.

covered by the highly elliptical RBSP orbits. Note that each panel presents over-plotted REPT-A and REPT-B data and the results seamlessly intercompare between the two instruments.

Figure 1 illustrates many important aspects of the relativistic electron record. The "three-belt" structure of the radiation zones during September 2012 is particularly clear in Figures 1c and 1d of the figure [see *Baker et al.*, 2013]. The "residual" nature of the storage ring that was persistently present up to $E > 8.8$ MeV is obvious in Figures 1c–1f. The abrupt cessation of the storage ring feature on 30 September (due to an interplanetary shock wave passage) is also clearly portrayed [see *Baker et al.*, 2013].

Other features evident in Figure 1 include the immensely powerful resurgence of the outer zone electron population on 9 October 2012: This reappearance of a new population of very high-energy electrons deep in the magnetosphere ($L = 4.0 \pm 0.5$) has been studied in detail by *Reeves et al.* [2013]. The October 2012 event was a clear illustration of the "local heating" mechanism for relativistic electron acceleration in the heart of the outer Van Allen belt and the physical processes involved have recently been well-modeled by *Thorne et al.* [2013b].

Following the strong October 2012 acceleration event, the dominant feature of the radiation belts at all of the energies portrayed in Figure 1 was one mostly of gradual relaxation and inward radial diffusion of the electrons (although several isolated abrupt outer zone depletion events occurred on 31 October 2012), in mid-November, and in mid-January. From the point of view of multi-MeV electrons, the dominant mode of behavior from ~1 November 2012 to ~1 March 2013 was one of "gradualism" and slow flux decay. From March 2013 to the end of the flux record (1 September 2013) in Figure 1, the magnetosphere became much more active compared to the prior four months with multiple examples of acceleration and large-scale transport at essentially all energies. Note that simply by visual inspection of Figure 1, the "three-belt" radiation zone structure seen in September 2012 is not an uncommon occurrence with clear examples being evident in March 2013, early April 2013, and again in late April to early May of 2013. The sensitivity and resolution of the REPT sensors make these morphological features stand out very clearly.

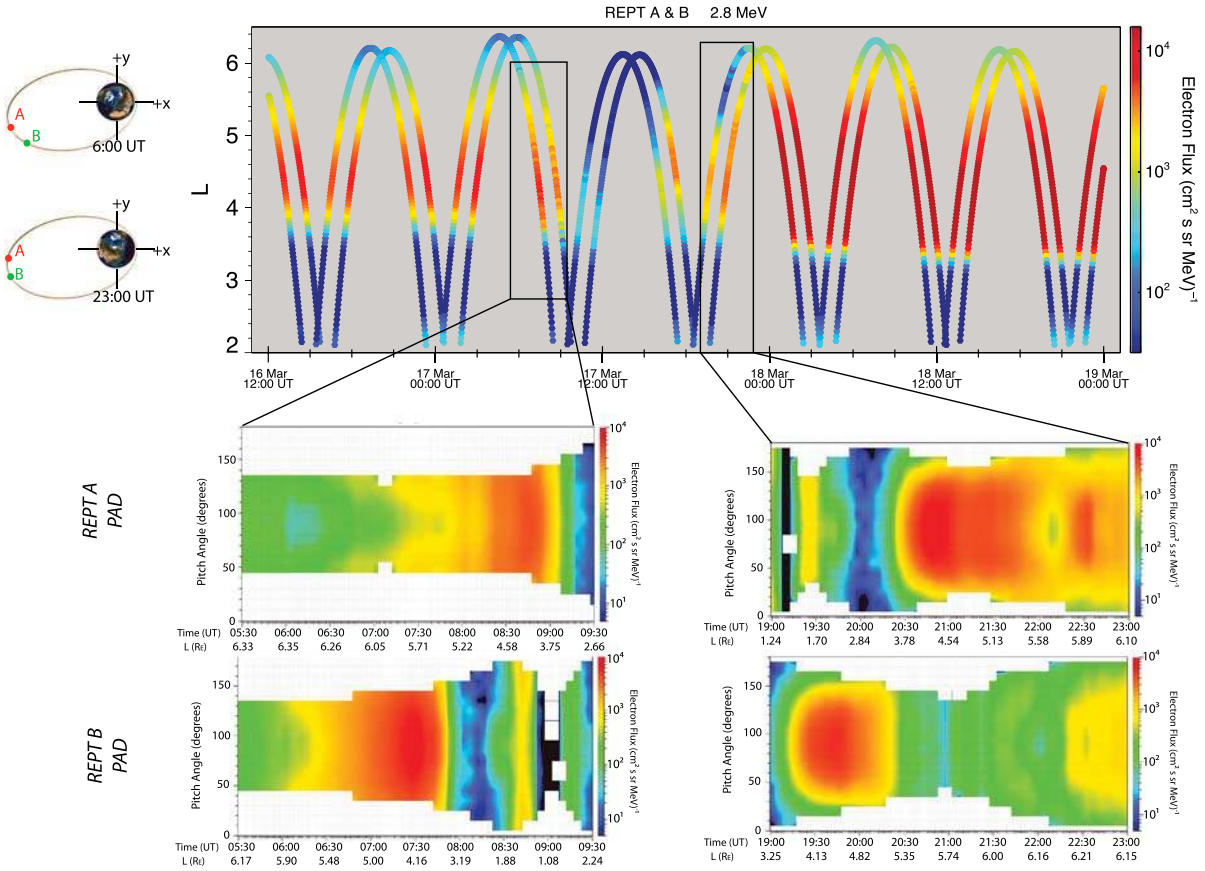

Figure 3. (top) Focused view of $E \sim 2.8$ MeV electron intensity (L versus time) for 16–18 March 2013 and (middle and bottom) detailed pitch angle distribution plots at selected times. The insets show a more limited pitch angle coverage at earlier times on 17 March—the direct result of a highly stretched magnetic field configuration during this time. Figure 3 (middle) corresponds to RBSP-A spacecraft measurements; Figure 3 (bottom) to RBSP-B measurements.

3. March 2013: A Remarkable Case Study Period

As is evident from Figure 1, the resurgence of radiation belt activity in March 2013—after a long and persistent relaxation of the system—was quite distinctive. The first half of the month (roughly) showed what appears to be a remarkable example of inward radial transport of electrons (see Figures 1a–1d): An enhancement in the lower energy channels, up to 5.6 MeV at larger L, occurred on March 1, and this will be discussed more later. There then appears to be an obvious line of demarcation on ~17 March where fluxes were reduced to essentially background levels (at higher energies) and a powerful new acceleration event then occurred (~18 March). This exhibited energization to levels discernible up to at least the $E = 7.2$ MeV channel (Figure 1e).

In Figure 2, we present REPT data for the entire month of March 2013 in a more detailed form. (Note that a somewhat different subset of REPT energy channels have been chosen for display in the five panels of Figure 2 as compared to Figure 1.) As seen readily in this figure, especially in Figures 2a–2c, the ~2.0–5.0 MeV electrons appeared suddenly on 1 March at relatively high L values (the peak fluxes being at L ~5 or higher, evident in Figure 1 as well). Over the course of the next 16 days, the relativistic electron fluxes followed an inward radial profile such that by early 17 March, the peak of absolute intensities (say for the $E = 4.5$ MeV channel, Figure 2c) was seen to be near $L = 4.0$. This appears to have been a textbook example of gradual and continuous inward radial diffusion [e.g., *Schulz and Lanzerotti*, 1974].

On 17 March at ~0600 UT, electron fluxes (both at REPT-A and REPT-B) were rapidly and dramatically depleted. This effect was particularly evident at high energies (see Figures 2c–2e), but was less complete at lower energies ($E < 3.0$ MeV). We have been able to trace the timeline of the causes of this particle depletion

quite thoroughly all the way back to the solar eruptions responsible: On 15 March, Active Region 1692 on the Sun produced a Class M1.1 X-ray flare at 0650 UT. A coronal mass ejection (CME) was detected by SOHO and STEREO imagers at 0654 UT propagating toward Earth with an initial speed of 1485 km/s. Subsequently, Advanced Composition Explorer (ACE) sensors detected a strong shock passage near the first Lagrangian (L1) point at 0528 UT on 17 March. This shock reached Earth's vicinity at 0604 UT on 17 March causing a strong geomagnetic storm sudden commencement (see Figure 4d) and almost immediate increases in auroral and ring current disturbance levels. The shock arrival caused rapid loss of multi-MeV electrons almost immediately, but by late on 17 March there was a huge reacceleration event that produced fresh electrons up to the $E = 7.2$ MeV energy range (see Figure 2e).

Having high time resolution measurements from the two spatially separated Van Allen Probe spacecraft allows us to examine rather precisely the loss and recovery of relativistic electrons on 17 March. Figure 3 shows, as a main panel, the highly resolved L versus time color-coded intensity plots for the REPT-A and REPT-B sensors (2.5–3.2 MeV). The relative spacecraft locations within the magnetosphere are shown by the small inset at the upper left of the diagram. The data demonstrate that in the period between ~1100 UT and ~1000 UT on 17 March, the outer electron belt was virtually annihilated. The small insets below the L versus time traces show (both at RBSP-A and RBSP-B locations) that the losses of the particles began after ~0600 UT by erosion of the 90° pitch angle electrons. This suggests probable loss of the electrons through drainage out of the magnetopause boundary [e.g., *Shprits et al*., 2006; *Turner et al*., 2012] coupled with energy-dependent radial transport due to drift shell splitting [e.g., *Wilken et al*., 1986]. The effect was larger (between 06:00 and 07:00 UT) at RBSP-A than at RBSP-B because RBSP-A was at a higher L location throughout this period.

The L versus time traces later in Figure 3 suggest that the acceleration and recovery of the 2.5–3.2 MeV electrons began by ~1800 UT on 17 March. Examination of similarly detailed plots (not shown here) for higher energy channels (see Figure 2, as well) shows that the $E > 4$ MeV electrons began their strongest recovery at ~2200 UT. As shown in detail in the accompanying paper by *Foster et al*. [2013], the powerful resurgence of multimegavolt electrons on 17 March corresponded closely to a strong substorm onset at 2215 UT. Certainly by early 18 March, the outer zone electron flux at energies above 2 MeV was 2 or more orders of magnitude higher than it had been prior to the flux dropout. The pitch angle information for both REPT-A and REPT-B (lower insets) in Figure 3 shows that a flux increase commenced essentially at the same time at both spacecraft locations (2220 UT). This was associated initially with electron enhancements near 90° pitch angles, which is consistent with local acceleration by chorus emissions [e.g., *Thorne et al*., 2013b; *Foster et al*., 2013].

Note that by using concurrent data from the Electric Field and Waves (EFW) experiment on board the RBSP spacecraft [see *Wygant et al*., 2013], we can continuously determine the plasmapause location throughout the period of these March 2013 observations. The black broken curve overplotted in Figure 2c shows this measured plasmaspheric outer boundary location as a function of time. It is seen that the plasmapause often traced the outer extent of the multi-MeV electron fluxes, but the plasmapause was driven briefly on both 1 March and on 17 March to very low L values (L ~2.5). It was during these specific times that electrons were strongly accelerated, probably by chorus wave interactions (as noted above). Thus, this shows that the extent of the plasmaspheric cold plasmas is intimately related to the spatial distribution and time evolution behavior of the outer zone energetic particle populations [cf., *Li et al*., 2006].

4. Phase Space Density and Solar Wind Forcing Properties

We know that changes in local magnetic field (B) properties within the magnetosphere can lead to apparent changes in high-energy particle fluxes. By computing the phase space density (PSD) at constant first $\left(\mu = \frac{p_\perp^2}{2m_o B}\right)$ and second $\left(K = I\sqrt{B_m}\right)$ adiabatic invariants [see *Reeves et al*., 2013; *Morley et al*., 2013] we can remove adiabatic effects leaving only the true particle acceleration (and loss) variations of the relativistic electron populations.

Figure 4a shows an example of PSD values for March 2013 calculated from REPT data, using the Tsyganenko (TS)04 magnetic field model [*Tsyganenko and Sitnov*, 2005], and plotted in L^* [see *Roederer*, 1970] versus time. In this plot the fixed μ value = 2878.6 MeV/G and the fixed K value = 0.1145 $R_E G^{1/2}$. The next lower panel shows a similar plot for μ =3433.3 MeV/G and the same K value. (Note that at geostationary orbit, $L = 6.6$, these μ values would, respectively, correspond to $E \sim 1.2$ MeV and $E \sim 1.5$ MeV electrons). The

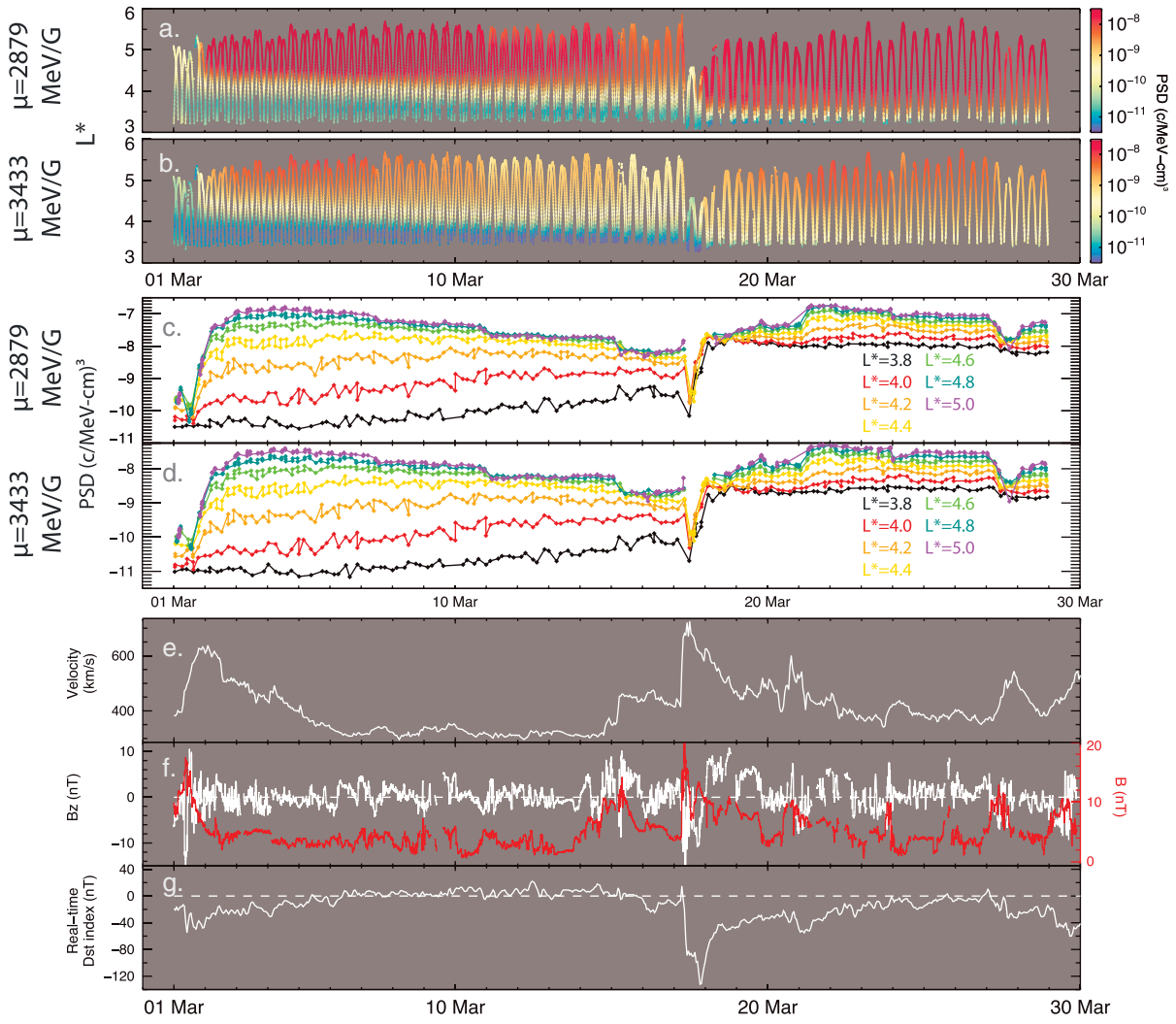

Figure 4. Electron phase space densities at constant μ and K: (a) $\mu = 2879$ MeV/G and (b) $\mu = 3433$ MeV/G). (c and d) Line plots at various fixed L^* values as indicated. (e) Solar wind speed, (f) IMF, and (g) *Dst* index for March 2013.

next panels down in Figures 4c and 4d) show "cuts" at various fixed L^* values in the form of line plots. The lowest three panels of Figure 4 show the concurrently measured upstream solar wind speed (in Figure 4e), the interplanetary magnetic field (IMF) magnitude (red) and IMF B_z component (white) (in Figure 4f), and the storm-time *Dst* index (in Figure 4g). Note on 1 March that a high-speed solar wind stream commenced, eventually reaching a peak solar wind speed of V ~650 km/s. There was no evidence of a shock during this time, and IMF strengths were fairly small. Hence, there was not a large *Dst* development in this case (Figure 4d). By contrast, on 17 March there was a strong interplanetary shock at ~0604 UT with a rapid increase of solar wind speed (V >700 km/s) and strong IMF enhancement. This led to *Dst* reaching ~ −130nT late on 17 March.

The PSD profiles in Figures 4a and 4b suggest that electron acceleration was rather gradual, particularly at lower L, in time from 1 March onward with peak phase space densities occurring several days after the solar wind stream leading edge passage. This is confirmed by the line plot profiles in Figures 4c and 4d. The data also hint that the highest PSD values were probably at (or somewhat beyond) the largest radial distances sampled by the RBSP spacecraft. Over time, the region of enhanced PSD tended to move gradually inward in L^* and overall, there was a weakening of the PSD strength, especially at lower L^* values, between early March and the deep outer zone depletion event on 17 March.

The PSD picture for the acceleration event on 17 March was different in character from that in early March. The data in Figures 4a and 4b show that the acceleration (i.e., enhanced PSD) late on17 March occurred initially centered on L^* ~4.0. The density enhancement was more abrupt than was the case for the high-speed stream event in early March. This point is made much more clear and quantitative by the line plot values shown in Figures 4c and 4d. Note also that a further increase of PSD occurred beginning on 21 March when V_{sw} increased and the *Dst* index was slightly enhanced. We, therefore, see that the two primary March 2013 radiation belt acceleration and transport events had several different characteristics owing to the substantially different solar wind/IMF drivers for the two cases.

5. Discussion and Conclusions

The first full year of Van Allen Probes observations demonstrate the immense benefits of near-equatorial dual-spacecraft measurements of highly relativistic electrons. Having excellent temporal, spatial, and energy resolution is key. The nearly equatorial orbit of Van Allen Probes allows them to observe particles at all equatorial pitch angles and allows the spacecraft to have a full view of the particle distribution. For extended periods of relative solar wind quiescence, the outer radiation belt can be characterized by slow, steady diffusive transport and gradual particle loss. However, appearance of enhanced solar wind forcing, as due to transient CME drivers or high-speed ($V > 500$ km/s) solar wind, quickly produces strong increases in particle fluxes (and concomitant increases in electron phase space densities). The Van Allen Probes observations have thoroughly reaffirmed and illuminated the intimate relationship between external solar wind forcing and internal magnetospheric particle acceleration and transport involving both solar wind streams [e.g., *Baker et al*., 1997] and involving CME-driven geomagnetic storms [e.g., *Baker et al*., 1998].

The March 2013 period represents a particularly important interval in which we see played out the workings of the Earth's "cosmic" accelerator. Results presented here show that an event early in March 2013 associated with a high-speed solar wind stream (but lacking an interplanetary shock or other such CME features) gave rise to a strong multi-MeV electron acceleration event that was "centered" at relatively large geocentric radial distances (r ~5–6 R_E). The population formed after the passage of the leading edge of a solar wind stream ($V \geq 650$ km/s) and for the next two weeks the core of the multi-MeV electron population was observed (see Figures 2 and 4) to diffuse inward in radial distance all the while exhibiting gradual diminution of phase space density, suggesting continual (weak) losses.

The products of the long diffusive acceleration event were largely and abruptly eradicated on 17 March 2013 by a strong interplanetary shock wave impacting the Earth's magnetosphere. In this shock passage, the solar wind speed jumped some 300 km/s (from ~425 km/s to ~725 km/s) and the IMF also showed very large changes. This led first to extensive radiation belt depletion but then led to almost as rapid a reappearance of a seemingly "new" radiation belt population very deep (L^* ~3-4) in the outer belt. This new population was very reminiscent of the October 2012 event examined by *Reeves et al*. [2013].

Concurrent observations from the EFW and Electric and Magnetic Field Instrument Suite and Integrated Science (EMFISIS) experiments on board the Van Allen Probes spacecraft show that both for the 1 March high-speed solar wind stream acceleration event and for the 17 March CME-driven acceleration event, the plasmapause boundary was forced deeply inward within the magnetosphere. Hence, we see that relativistic electron acceleration occurs when (and perhaps only when?) the outer zone is situated well outside the plasmasphere and chorus-mode waves beyond the plasmapause can interact with the substorm- generated "seed" particles [see *Baker and Kanekal*, 2008] that are necessary for relativistic electron production. The details of this acceleration process for 17–18 March 2013 as it relates to the plasmaspheric configuration and wave properties are explored in the companion paper by *Foster et al*. [2013].

Acknowledgments

This work was supported by JHU/APL contract 967399 under NASA's prime contract NAS5-01072. All Van Allen Probes data used are publicly available at (www.rbsp-ect.lanl.gov).

The Editor thanks two anonymous reviewers for their assistance in evaluating this paper.

References

Baker, D. N., and J. B. Blake (2012), SAMPEX, A long-serving radiation belt sentinel, in *Dynamics of the Earth's Radiation Belts and Inner Magnetosphere*, Geophys. Monogr. Ser., vol. 199, 21 p., AGU, Washington, D. C., doi:10.1029/GM199.

Baker, D. N., and S. G. Kanekal (2008), Solar cycle changes, geomagnetic variations, and energetic particle properties in the inner magnetosphere, *J. Atmos. Sol. Terr. Phys.*, *70*, 195–206.

Baker, D. N., et al. (1997), Recurrent geomagnetic storms and relativistic electron enhancements in the outer magnetosphere: ISTP coordinated measurements, *J. Geophys. Res.*, *102*(A7), 14,141–14,148.

Baker, D. N., T. I. Pulkkinen, X. Li, S. G. Kanekal, J. B. Blake, R. S. Selesnick, M. G. Henderson, G. D. Reeves, H. E. Spence, and G. Rostoker (1998), Coronal mass ejections, magnetic clouds, and relativistic magnetospheric electron events: ISTP, *J. Geophys. Res.*, *103*(A8), 17, 279–17, 291.

Baker, D. N., et al. (2012), The Relativistic Electron-Proton Telescope (REPT) instrument on board the Radiation Belt Storm Probes (RBSP) spacecraft: Characterization of Earth's radiation belt high-energy particle populations, *Space Sci. Rev.*, doi:10.1007/s11214-012-9950-9.

Baker, D. N., et al. (2013), A long-lived relativistic electron storage ring embedded in Earth's outer Van Allen belt, *Science*, *340*, 186–190, doi:10.1126/science.1233518.

Foster, J. C., et al. (2013), Prompt energization of relativistic and highly relativistic electrons during a substorm interval: Van Allen Probes observations, *Geophys. Res. Lett.*, doi:10.1002/2013GL058438.

Li, X., D. N. Baker, P. O'Brien, L. Xie, and Q. G. Zong (2006), Correlation between the inner edge of outer radiation belt electrons and the innermost plasmapause location, *Geophys. Res. Lett.*, *33*, L14107, doi:10.1029/2006GL026294.

Mauk, B. H., N. J. Fox, S. G. Kanekal, R. L. Kessel, D. G. Sibeck, and A. Ukhorskiy (2012), Science objectives and rationale for the Radiation Belt Storm Probes mission, *Space Sci. Rev.*, doi:10.1007/s11214-012-9908-y.

Morley, S. K., M. G. Henderson, G. D. Reeves, R. H. W. Friedel, and D. N. Baker (2013), Phase space density matching of relativistic electrons using the Van Allen Probes: REPT results, *Geophys. Res. Lett.*, *40*, 4798-4802, doi:10.1002/grl.50909.

Reeves, G. D., et al. (2013), Electron acceleration in the heart of the Van Allen radiation belts, *Science*, *341*, 999–994, doi:10.1126/science.1237743.

Roederer, J. G. (1970), *Dynamics of Geomagnetically Trapped Radiation*, Springer-Verlag, New York.

Schulz, M., and L. J. Lanzerotti (1974), *Particle Diffusion in the Radiation Belts*, Springer-Verlag, New York.

Shprits, Y. Y., R. M. Thorne, R. Friedel, G. D. Reeves, J. Fennell, D. N. Baker, and S. G. Kanekal (2006), Outward radial diffusion driven by losses at magnetopause, *J. Geophys. Res.*, *111*, A11214, doi:10.1029/2006JA011657.

Shprits, Y. Y., D. Subbotin, A. Drozdov, M. E. Usanova, A. Kellerman, K. Orlova, D. N. Baker, D. L. Turner, and K.-C. Kim (2013), Unusual stable trapping of the ultra-relativistic electrons in the Van Allen radiation belts, *Nat. Phys.*, doi:10.1038/nphys2760.

Thorne, R. M., et al. (2013a), Evolution and slow decay of an unusual narrow ring of relativistic electrons near L ~3.2 following the September 2012 magnetic storm, *Geophys. Res. Lett.*, *40*, 1–5, doi:10.1002/grl.50627.

Thorne, R. M., et al. (2013b), Rapid local acceleration of relativistic radiation belt electrons by magnetospheric chorus, *Nature*, *504*, 411–414, doi:10.1038/nature12889.

Tsyganenko, N. A., and M. L. Sitnov (2005), Modeling the dynamics of the inner magnetosphere during strong geomagnetic storms, *J. Geophys. Res.*, *110*, A03208, doi:10.1029/2004JA010798.

Turner, D. L., Y. Y. Shprits, M. Hartinger, and V. Angelopoulos (2012), Explaining sudden losses of outer radiation belt electrons during geomagnetic storms, *Nat. Phys.*, *8*, 208–212, doi:10.1038/nphys2185.

Van Allen, J. A., et al. (1958), Observation of high intensity radiation by satellites 1958 Alpha and Gamma, *Jet Propuls.*, *28*, 588–592.

Wilken, B., D. N. Baker, P. R. Higbie, T. A. Fritz, W. P. Olson, and K. A. Pfitzer (1986), Magnetospheric configuration and energetic particle effects associated with a SSC: A case study of the CDAW 6 Event on March 22, 1979, *J. Geophys. Res.*, *91*(A2), 1459–1473, doi:10.1029/JA091iA02p01459.

Wygant, J. R., et al. (2013), The Electric Field, and Waves (EFW) instruments on the Radiation Belt Storm Probes Mission, *Space Sci. Rev.*, doi:10.1007/s1124-013-0013-7.